Thermodynamic Reciprocity of the Inhibitor Binding to the Active Site and the Interface Binding Region of IB Phospholipase A2

Otto G. Berg,*,‡ Bao-Zhu Yu,§ and Mahendra K. Jain*,§

Department of Molecular Evolution, Uppsala University Evolutionary Biology Center, Uppsala, Sweden, and Department of Chemistry and Biochemistry, University of Delaware, Newark, Delaware 19716

Received July 2, 2008; Revised Manuscript Received December 30, 2008

ABSTRACT: Interfacial activation of pig pancreatic IB phospholipase A_2 (PLA2) is modeled in terms of the three discrete premicellar complexes ($E_i^{\#}$, $i = 1$, 2, or 3) consecutively formed by the cooperative binding of a monodisperse amphiphile to the i-face (the interface binding region of the enzyme) without or with an occupied active site. Monodisperse PCU, the *sn*-2-amide analogue of the zwitterionic substrate, is a competitive inhibitor. PCU cooperatively binds to the i-face to form premicellar complexes ($\tilde{E}_i$, $i = 1$ or 2) and also binds to the active site of the premicellar complexes in the presence of calcium. In the $\tilde{E}_i$I complex formed in the presence of PCU and calcium, one inhibitor molecule is bound to the active site and a number of others are bound to the i-face. The properties of the $\tilde{E}_i$ complexes with PCU are qualitatively similar to those of $E_i^{\#}$ formed with decylsulfate. Decylsulfate binds to the i-face but does not bind to the active site in the presence of calcium, nor does it interfere with the binding of PCU to the active site in the premicellar complexes. Due to the strong coupling between binding at the i-face and at the active site, it is difficult to estimate the primary binding constants for each site in these complexes. A model is developed that incorporates the above boundary conditions in relation to a detailed balance between the complexes. A key result is that a modest effect on cooperative amphiphile binding corresponds to a large change in the affinity of the inhibitor for the active site. We suggest that besides the binding to the active site, PCU also binds to another site and that full activation requires additional amphiphiles on the i-face. Thus, the activation of the inhibitor binding to the active site of the $E_2^{\#}$ complex or, equivalently, the shift in the $E_1^{\#}$ to $E_2^{\#}$ equilibrium by the inhibitor is analogous to the allosteric activation of the substrate binding to the enzyme bound to the interface.

Three contributions increase the processive interfacial catalytic turnover rate of secreted pig pancreatic IB phospholipase A_2 (PLA2)[1] on bilayers and micelles. First, the high-affinity binding of PLA2 to the anionic interface along its interface binding surface, the i-face, increases the residence time of the interface-activated E* for the processive interfacial turnover (*1*−*4*). Second, K_S* activation (*5, 6*), or enhanced substrate affinity, allows the active site of E* to bind the substrate 10−100-fold more strongly compared to the solution form (E). Third, ∼100-fold k_{cat}* activation is attributed to the enzyme binding to the zwitterionic interface, and an additional 40-fold activation if the interface is anionic (*7, 8*).

* To whom correspondence should be addressed. Telephone: (302) 831-2968. Fax: (302) 831-6335. E-mail: mkjain@udel.edu.

‡ Uppsala University Evolutionary Biology Center.

§ University of Delaware.

[1] Abbreviations: CMC, critical micellization concentration of a single amphiphile; IMC, CMC of the amphiphile in the presence of a constant concentration of another amphiphile; DC_7PC, diheptanoyl-3-phosphatidylcholine; DMPM, dimyristoylphosphatidylmethanol; i-face, interface binding surface of an interfacial enzyme; MG14, L-1-*O*-octyl-2-heptylphosphonyl-*sn*-glycero-3-phosphoethanolamine; MJ33, 1-hexadecyl-3-(trifluoroethyl)-*rac*-glycero-2-phosphomethanol; MJ72, 1-octyl-3-(trifluoroethyl)-*rac*-glycero-2-phosphomethanol; PCU, 2-dodecanylaminohexanol-2-phosphocholine; PGU, 2-dodecanylaminohexanol-2-phosphoglycol; PLA2, secreted 14 kDa type IB phospholipase A_2 from pig pancreas; RET, fluorescence resonance energy transfer; TMA-DPH, trimethylammonium diphenylhexatriene.

Scheme 1

$$E \underset{n_1, K_1^{\#}}{\overset{+N_1\,A}{\rightleftharpoons}} E_1^{\#} \underset{n_2, K_2^{\#}}{\overset{+N_2\,A}{\rightleftharpoons}} E_2^{\#} \underset{n_3, K_3^{\#}}{\overset{+N_3\,A}{\rightleftharpoons}} E_3^{\#}$$

Characterization of the individual interface-bound forms of PLA2 is challenging. In this and the next paper, we employ an alternative strategy that extends the interfacial kinetic paradigm for PLA2 (*9, 10*) to model the functional properties of its premicellar complexes (Scheme 1). Two thermodynamic expectations are of interest. The first relates to the interfacial binding, and the second relates to the interfacial activation. The expectation for an interfacial enzyme is that since its i-face is designed to bind to the organized interface of an amphiphile aggregate, the i-face will also tend to organize and cooperatively bind the headgroups of monodisperse amphiphiles to form premicellar complexes (*11*−*14*). Thus, the $E_i^{\#}$ complexes are possible surrogates for the functional states of the interface-bound enzyme, and the underlying parameters are proxies for the interfacial steps.

As shown in Scheme 1, three discernible premicellar $E_i^{\#}$ ($i = 1$, 2, or 3) complexes of PLA2 are formed with monodisperse decylsulfate (*15, 16, 11, 17*) which does not bind to the active site. $E_i^{\#}$ complexes are sequentially formed by contiguous binding of additional N_i amphiphiles per enzyme to the i-face with Hill number n_i and dissociation

10.1021/bi801244u CCC: $40.75
Published on Web 03/20/2009

constant $K_i^{\#}$ (*11, 14*). Characterization of the inhibitor binding to the i-face in the $E_i^{\#}$ complexes is possible because the amphiphile binding to the i-face does not require calcium (*14*), whereas the inhibitor binding to the active site of E, E*, or $E_i^{\#}$ obligatorily requires calcium (*18*). This permits analysis of the second thermodynamic expectation of the reciprocity between the i-face and active site binding (*5*). We present strategies to extend Scheme 1 for the amphiphile binding to the i-face by including steps for the separate binding of the inhibitor to the active site of PLA2 in the presence of calcium. The resulting models are useful for analyzing binding to the i-face and to the active site in the premicellar complexes. Since binding to the active site can be assessed only under certain conditions, changes in cooperative binding to the i-face are used to infer active site events.

We characterize the binding of inhibitor amphiphiles to PLA2 in the presence or absence of calcium to gain insight into interfacial activation (*5*−*7*). The results show that the amphiphile binding affinity for the i-face of the complex is enhanced if an inhibitor is bound to the active site. Conversely, the binding affinity of inhibitor I for the active site in EI is significantly lower than its affinity in the premicellar $E_i^{\#}I$ complexes. This thermodynamic reciprocity between the active site and cooperative i-face interactions is most prominent in the $E_1^{\#}$ to $E_2^{\#}$ step. The relationship of this step to interfacial activation for the formation of the E*S Michaelis complex and the chemical step is also considered. In the following paper (*19*), the structural basis for the interfacial activation is elaborated in terms of the classical T (inactive) to R (active) allosteric transition.

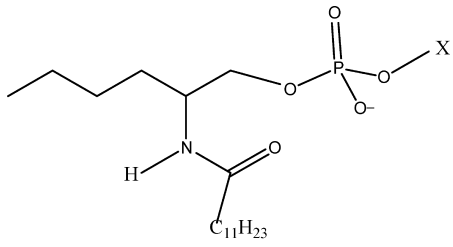

PCU, X= - CH_2-CH_2-$N^+(CH_3)_3$ (choline)

PGU, X = -CH_2CH_2OH (glycol)

EXPERIMENTAL PROCEDURES

PCU and PGU were provided by M. J. W. Janssen (Utrecht, The Netherlands). Other reagents, methods, protocols, and precautions for characterizing the binding of monodisperse amphiphiles to the i-face and the active site of PLA2 are as described previously (*11, 13, 20*). Specific experimental details, models, and interpretations are given in the figure legends and the text. The CMC determined by the surface balance method (*11*) is ~200 μM for PCU, PGU, or MG14, 700 μM for MJ72, and 9 μM for MJ33. In a mixture of amphiphiles, the intermicellar concentration (IMC) decreases noticeably due to an intermolecular association equilibrium that depends on the relative concentrations of the amphiphiles. Our measurements, at least up to 2500 μM decylsulfate whose CMC is 4500 μM, were carried out at the inhibitor concentrations at which, based on the surface pressure measurements, mixed micelles or comicelles are not present.

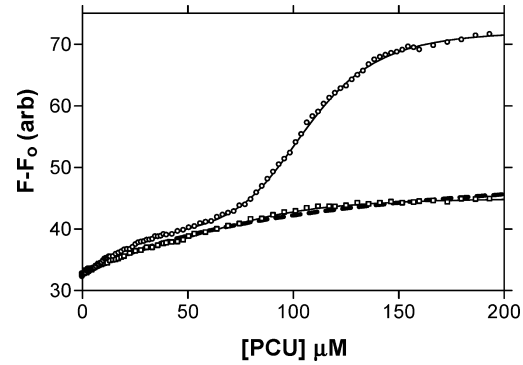

FIGURE 1: Monodisperse PCU concentration (CMC = 0.220 mM) dependence of the change in the relative fluorescence intensity (emission at 333 nm, excitation at 280 nm) from Trp-3 of 1 μM PLA2 in pH 6.9 buffer containing (□) EGTA or (○) 0.5 mM $CaCl_2$. Parameters for the fit (solid line) to Scheme 2 are discussed in the Appendix. The fit to a single hyperbola with a K_1 of 109 μM is shown as a dashed bold line.

Monodisperse Amphiphile Binding to PLA2. Experimental protocols, theory, and interpretation of the cooperative decylsulfate binding model in Scheme 1 are established and described in detail for the binding of decylsulfate (*11, 14*), and additional details are given in the text and figure captions. Amphiphile binding to the i-face of PLA2 is accompanied by an increase in the fluorescence emission signal intensity from Trp-3. The fluorescence increase from 1 or 2 μM PLA2 with the amphiphile concentration was monitored on an SLM-Aminco AB2 instrument set in the ratio mode with 4 nm slit widths with excitation at 280 nm and emission at 333 nm for the Trp signal, or at 450 nm for the RET signal from the Trp/TMA-DPH pair. Intensity values obtained with an integration time of 4 s have a noise level of <1%. Controls with the W3F mutant of PLA2 showed that more than 97% of the reported signal intensity changes are from Trp-3. Measurements at pH 6.9 were taken in 10 mM HEPES, 10 mM Tris, 0.48 M NaCl, and 0.5 mM calcium or 1 mM EGTA with 1 mM EDTA.

Typically, for the analysis of the Trp signal with Scheme 1, it is convenient to consider the relative changes in signal as $\delta F = F/F_0 - 1$, where F is the signal at the given decylsulfate concentration and F_0 the one at concentration zero; this automatically compensates for small variations in the background signal. For the more complex schemes, where the ground state is a mixture of different binding states with different signals, reformulating the equations to describe the relative changes in signal only makes calculations more difficult without any obvious gain. In such cases, e.g., Figures 1 and 5, to make the curves level off at the same value at low I and/or decylsulfate, as required by the models, for some curves all intensity data points are adjusted (by adding or subtracting a constant value). This corresponds to a small (<5%) shift in the background signal which could be due to calcium binding or simply to uncertainties in the background signal.

Inhibitor Binding Constant Determined by the Protection Method. The half-time for alkylation of catalytic residue His-48 of PLA2 by *p*-nitrophenacyl bromide is more than 30-fold longer if the active site of PLA2 in the E, $E_i^{\#}$, or E* form is occupied by calcium alone or by an inhibitor (*18, 21*). The protection measured as the increase in the half-time provides a reliable quantitative basis for the determination

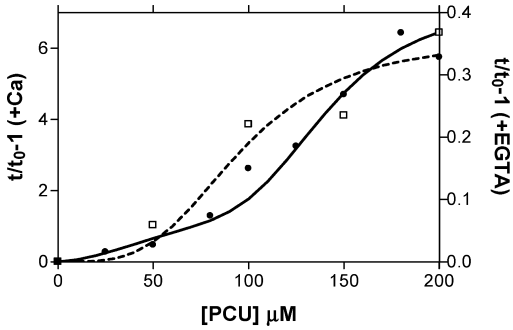

FIGURE 2: PCU concentration dependence of the relative inactivation time of PLA2 by *p*-nitrophenacyl bromide in pH 6.9 buffer containing (white symbols with the right *Y*-axis) EGTA and EDTA or (black symbols with the left *Y*-axis) 0.5 mM calcium. Lines are fits for the model in Scheme 2 obtained with the fit parameters given in the Appendix. Uncertainty in individual data points is <10%.

Scheme 2

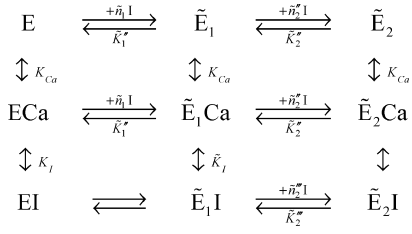

Scheme 3

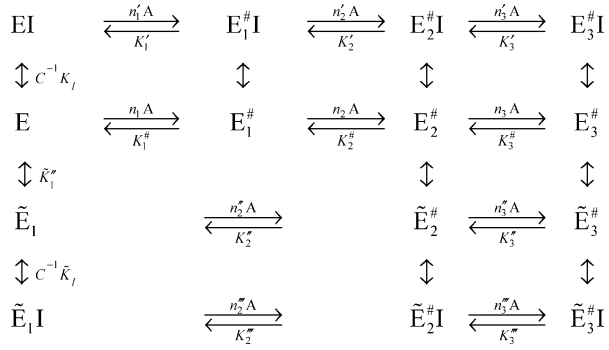

of the dissociation constant of calcium and the inhibitor. The relative increase in the alkylation time is proportional to the fraction of enzymes with an occupied active site. Specific analytical protocols for the interpretation of the alkylation times and the extent of protection of the premicellar complexes are developed below.

RESULTS

In this paper, we extend Scheme 1 to include models for analysis of curves for amphiphile binding to the $E_i^{\#}$ complexes of PLA2 in the presence of calcium and inhibitor. Here the analytical strategy is to include in the model all functionally defined states that may exist under the experimental conditions and may be associated with the interfacial activation. The resulting paradigm shown in Schemes 2 and 3 is far too complex to permit analysis of each elementary step. Assumptions and quantitative analysis of the models and uncertainties in the fit parameters for the experimental results are discussed in the Appendix. From the detailed fits, it is possible to show that the results are consistent with the model. However, in this section, we will focus primarily on the qualitative interpretation of the results.

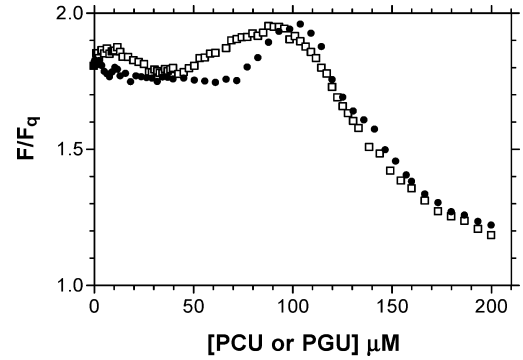

FIGURE 3: PCU (●) or PGU (□) concentration-dependent change in the F/F_q ratio for Trp-3 of PLA2 in 0.5 mM $CaCl_2$ buffer at pH 6.9. F is the fluorescence intensity of the enzyme alone, and F_q is the intensity in the presence of 0.15 M succinimide quencher. The F/F_q ratio decreases because F_q is higher when Trp-3 is shielded by the bound amphiphile cluster. Comparable results were also obtained in the absence of calcium (not shown).

Premicellar Complexes with Inhibitor Amphiphiles. Both zwitterionic PCU and anionic PGU are potent active site-directed inhibitors of PLA2 (*22, 23*) with $X_I(50)$* representing 50% inhibition of the processive turnover on DMPM vesicles at 0.004 mole fraction for PCU and at 0.001 mole fraction for PGU (*21*). The calcium-dependent binding of inhibitors to the active site of PLA2 is significantly stronger for the interface-bound E* form than for the E form in the aqueous phase (*5, 9, 10*). In fact, there is considerable uncertainty about whether a true dissociation constant for the EI complex in the aqueous phase can be determined. Also, it is not clear if catalytic turnover occurs at all via the Michaelis−Menten ES complex in the aqueous phase in the presence of the monodisperse substrate alone (*24*). Such concerns are supported by results below which also show that zwitterionic PCU forms premicellar complexes with PLA2 with or without a PCU molecule bound to the active site.

As shown in Figure 1, binding of monodisperse zwitterionic PCU to PLA2 induces a significant change in the Trp-3 emission intensity at 333 nm both in the presence and in the absence of calcium. As shown for the micelle and bilayer interfaces, the Trp-3 signal changes with the binding of the enzyme to the interface, and the signal changes little with the occupancy of the active site (*5, 25*). Thus, the fluorescence intensity change in Figure 1 is largely due to the binding of monodisperse PCU to the i-face. Calcium, when present, binds to the catalytic site in a manner independent of the i-face events. Calcium binding as such does not significantly (<5%) influence the Trp-3 emission from E (*19*), and possibly not from the other complexes, including the premicellar complexes with decylsulfate alone (*11, 20*). Thus, the additional effect of calcium on the titration curve with PCU is attributed to the effect of PCU binding at the active site on the PCU binding at the i-face. In the Appendix, these titration curves are quantitatively analyzed and interpreted in terms of Scheme 2. It is an extension of Scheme 1 with the difference being that $E_i^{\#}$ with decylsulfate is replaced by $\tilde{E}_i$ for the corresponding premicellar complexes with PCU, and the steps are added for the calcium-dependent binding of PCU to the active site.

In the presence of calcium, the titration curve is clearly biphasic, and it is very similar to the corresponding curves

for the titration with decylsulfate with or without calcium (*11, 20*). The curve in Figure 2 corresponds to the formation of two consecutive complexes. The first step has a low Hill number (~1), possibly corresponding to the binding of one PCU to a single site. This is followed by the cooperative binding (clustering) of a number of PCU molecules with a Hill number of ~6−8. In contrast, the curve with EGTA in Figure 1 looks nearly hyperbolic, suggestive of a single binding step with a Hill number of ~1. This would imply a very strong cooperativity between the i-face and active site such that the second premicellar complex ($\tilde{E}_2$) with PCU can form only after calcium and PCU are bound at the active site. However, in analogy with the behavior with decylsulfate (*11, 15−17, 20*), a two-step binding seems likely also in the absence of calcium. This leads to a significant improvement in the fit, and the mean-square deviation between data points and the best-fit curve decreases by a factor of 5. Also, other results, e.g., the RET experiments discussed below, support a two-step binding, including clustering of PCU also in the absence of calcium.

Figure 1 shows that PCU alone forms premicellar complexes on the i-face of PLA2 and that this i-face binding can have a strong effect on the affinity of PCU for the active site. This is supported by the protection results in Figure 2 which are also quantitatively interpreted in terms of the model in Scheme 2. The calcium-dependent inhibitor binding to the active site increases the alkylation time of H48. The relative rate of alkylation as a function of the inhibitor concentration is a reliable measure of its affinity for the active site (*18, 21, 26*), and the sigmoidal shape suggests a cooperative process. The decrease in the rate of alkylation of H48 is due to the binding of calcium at the catalytic site, and the apparent affinity of the calcium increases by sequential binding of an active site-directed inhibitor. In the presence of Ca, the best fit for the curve in Figure 2 as shown is with a K_I of 300 μM. Reducing K_I below 50 μM significantly impairs the fit at low PCU concentrations, unless it can be argued that the binding of inhibitor to form the EI complex somehow greatly weakens the protection afforded by the bound calcium.

The best fits for the data in Figures 1 and 2 to Scheme 2 suggest a two-step binding, including inhibitor clustering, on the i-face of PLA2 and that this i-face binding is cooperative with binding at the active site. The strongest support for a two-step binding, including the clustering of PCU in $\tilde{E}_2$, also in the absence of calcium, comes from the experiments discussed next.

Clustering of the Inhibitor Amphiphile in the Premicellar $\tilde{E}_2$ and $\tilde{E}_2$I Complexes. The Hill cooperativity for the formation of $\tilde{E}_1$ and $\tilde{E}_2$ complexes is consistent with independent results that show clustering of PCU around Trp-3 in $\tilde{E}_2$ and $\tilde{E}_2$I but not in $\tilde{E}_1$ or $\tilde{E}_1$I. As shown in Figure 3, above 0.11 mM PCU or PGU, Trp-3 on the i-face is shielded from 0.15 M succinimide in the aqueous phase. Thus, Trp-3 is shielded in $\tilde{E}_2$I, and the shielding in E, $\tilde{E}_1$, or $\tilde{E}_1$I is similar to that for Trp on the protein surface (*27, 28*). Note that between 0.08 and 0.11 mM PCU, the level of quenching decreases marginally as if Trp-3 in $\tilde{E}_1$ or $\tilde{E}_1$I is somewhat more accessible to aqueous succinimide.

Additional evidence for the clustering of PCU is shown in Figure 4 where the fluorescence RET signal intensity from TMA-DPH bound to PLA2 changes with the PCU concentration. Both in the presence and in the absence of calcium, the intensity decreases up to 0.05 mM PCU and then increases at the higher concentrations. In analogy with the results with decylsulfate (*11, 17*), the initial quenching and saturation of the signal above the complete quenching level suggest that TMA-DPH remains bound to $\tilde{E}_1$ and $\tilde{E}_1$I, albeit with a significant difference in the RET signal intensity. The signal intensity increases again as the probe partitions in the cluster of the PCU molecules around Trp-3 in $\tilde{E}_2$. Note that this increase in the magnitude of the RET signal is observed in the absence of calcium where a cooperative change in the Trp-3 signal is expected from $\tilde{n}_2'' = 2$ to 5 for $\tilde{E}_2$, as well as in the presence of calcium where $\tilde{n}_2 = 6-8$ for $\tilde{E}_2$I (Figure 1). Independent controls with micelles of PCU showed that most of the intensity increase in Figure 4 above 0.1 mM is due to the resonance energy transfer signal, and the partitioning of TMA-DPH in the PCU cluster in $\tilde{E}_2$ and $\tilde{E}_2$I may contribute no more than 20% of the intensity increase. Together, the biphasic quenching in Figure 3 and the biphasic RET behavior in Figure 4 with PCU are qualitatively comparable to that observed with decylsulfate and show that PCU amphiphiles bound to $\tilde{E}_2$ and $\tilde{E}_2$I are clustered around Trp-3.

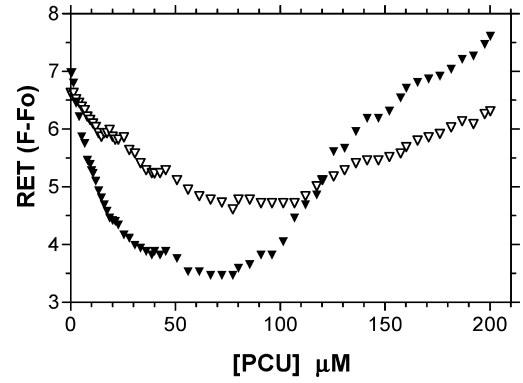

FIGURE 4: PCU concentration-dependent change in the RET signal intensity (excitation at 280 nm and emission at 450 nm) from 1 μM TMA-DPH and 1 μM PLA2 in buffer at pH 6.9 containing (▽) 1.3 mM EGTA or (▼) 2 mM $CaCl_2$.

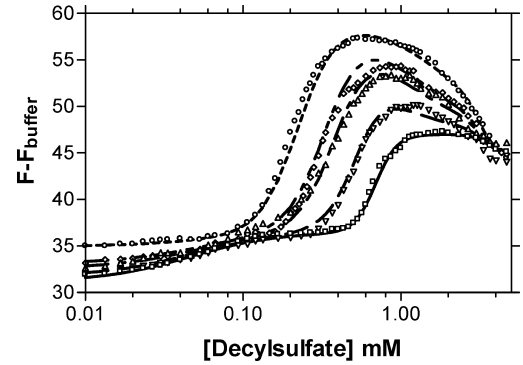

FIGURE 5: Trp signal from 2 μM PLA2 with decylsulfate titration at pH 6.9 with 0, 2, 5, 7, and 15 μM PCU, from bottom to top, respectively. Fit (lines) parameters to Scheme 3 as developed in the Appendix are summarized in Table 1.

Effect of PCU on Decylsulfate Binding to PLA2. The calcium-dependent affinity of decylsulfate for the active site of the $E_i^{\#}$ complexes is poor (*11, 14*). It permits study of PCU binding to the $E_i^{\#}$ complexes of decylsulfate as shown in Figure 5. However, the interpretation is complicated because PCU and decylsulfate may compete or cooperate

Table 1: One Set of Possible Fit Parameters[a] at pH 6.9 from the Application of Schemes 2 and 3 to the Experimental Data in Figures 1 and 5

$A_0^I = 43$	$n_1' = 1.5$	$A_1^I = 36$	$n_2' = 6$	$A_2^I = 50$	$n_3' = 9$	$A_3^I = 40$
$K_1 = 300$	$K_1' = 46$		$K_2' = 280$		$K_3' = 3.7$	
$A_0 = 31.2$	$n_1 = 1.6$	$A_1 = 36.5$	$n_2 = 6$	$A_2 = 47$	$n_3 = 9$	$A_3 = 45$
$K_1'' = 44$	$K_1^{\#} = 46$		$K_2^{\#} = 690$		$K_3^{\#} = 2800$	
$\tilde{n}_1 = 1$						
$B_1 = 42$			$n_2'' = 5$	$B_2 = 52$	$n_3'' = 9$	$B_3 = 45$
$\tilde{K}_1 = 24$			$K_2'' = 200$		$K_3'' = 3000$	
$B_1^I = 42$			$n_2''' = 5$	$B_2^I = 59$	$n_3''' = 9$	$B_3^I = 50$
			$K_2''' = 88$		$K_3''' = 2900$	

[a] All dissociation constants in this table are expressed in micromolar.

for binding at the i-face. As developed and interpreted in the Appendix, analyses of results in Figure 5 show that binding of one PCU to the active site and of another to the i-face is promoted by the binding of decylsulfate to the i-face. Apparent intensity values are also higher in the presence of PCU which is consistent with an effect of PCU on the short-range specific interactions along the i-face (*11*). The fits shown in Figure 5 were obtained with three simplifying assumptions using the binding states in Scheme 3. First, on the basis of the similarity between the first i-face binding states of PCU ($\tilde{E}_1$) and decylsulfate ($E_1^{\#}$), it is assumed that they form on the same site and are mutually exclusive. Second, at low concentrations, PCU does not participate in (or hinder) the decylsulfate clustering in $E_2^{\#}$ or $E_3^{\#}$; however, decylsulfate can bind to the i-face of $\tilde{E}_1$ (with PCU) to form the mixed states $\tilde{E}_2^{\#}$ and $\tilde{E}_3^{\#}$. Third, the effect of calcium is only on the binding of PCU to the active site.

The most obvious effect of increasing the amount of PCU in Figure 5 is the shift in the formation of $E_2^{\#}$ to lower concentrations of decylsulfate, which shows that binding of PCU increases the affinity for decylsulfate in the premicellar complexes. The converse is also true by thermodynamic reciprocity, i.e., formation of $E_2^{\#}$ or $\tilde{E}_2^{\#}$ increases the affinity for PCU. There are in principle two ways to achieve this cooperativity: Either there is a general cooperativity between the i-face and the active site such that binding of any amphiphile at either site increases the affinity for the other, or there is a specific PCU effect such that binding of PCU to the i-face ($\tilde{E}_1$) strengthens both the formation of $\tilde{E}_2^{\#}$ with decylsulfate and also the PCU binding in the active site. The experimental data in Figure 5 do not allow a distinction between these alternatives, and similarly good fits could be achieved with various combinations of these basic alternatives, as discussed in the Appendix. As shown in Figure 6, the different fits lead to different predictions for the expected affinity of the active site as being dependent on the amount of decylsulfate, although the overall behavior is qualitatively similar and multiphasic.

Premicellar Complexes of Anionic Inhibitors. The emission intensity of E* on the bilayer vesicles (*25*) and of the $E_i^{\#}$ complexes (Figures 1 and 5) depends on the amphiphile headgroup. This is attributed to an effect of short-range specific interactions of the amphiphile head groups for ligand substitution along the i-face which is necessary for its desolvation (*29*−*31*). Also, in the titration curves for PLA2 with several competitive inhibitors (not shown), the monomer concentration-dependent increase in the Trp-3 emission depends on the calcium concentration and the structure of the inhibitor. These titration curves were not characterized further. However, decylsulfate titration curves in the presence of 2 μM PGU, MJ33, and MG14 are shown in Figure 7A,

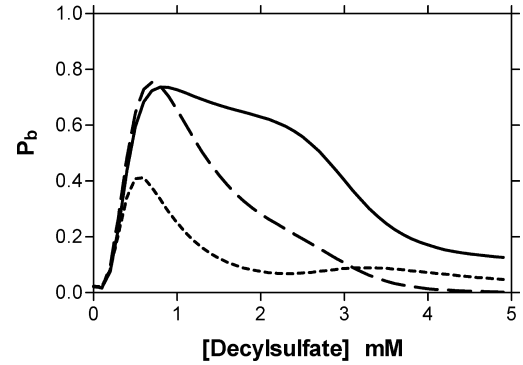

FIGURE 6: Binding probability of PCU at the catalytic site, as a function of the concentration of decylsulfate calculated from Scheme 3 at 5 μM PCU and 0.5 mM calcium. As developed in the Appendix, the different curves are for different assumptions about the cooperativity between i-face and active site binding.

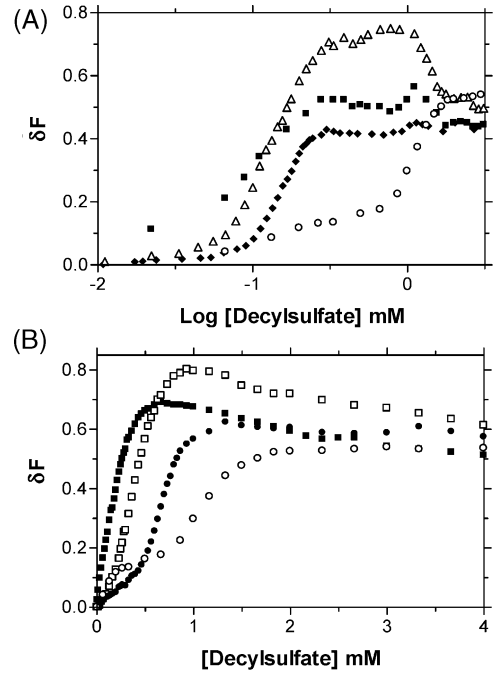

FIGURE 7: (A) Decylsulfate concentration dependence of the normalized Trp-3 emission intensity of 2 μM PLA2 (○) alone and with (■) 2 μM MJ33, (△) 2 μM PGU, or (◆) 2 μM MG14 at pH 8.0 and 0.5 mM Ca. (B) Effect of (from right to left) 0 (○), 10 (●), 50 (□), and 100 μM MJ72 (■) on the decylsulfate binding curves of 2 μM PLA2 in 0.5 mM Ca at pH 8.0.

and the effect of the concentration of MJ72 on the decylsulfate titration curve is shown in Figure 7B. Qualitatively, these titration curves are similar to those in Figure 5: the presence of inhibitor shifts the appearance of the premicellar complexes to lower decylsulfate concentrations. However, these curves could not be fitted well in Scheme 3, and fits

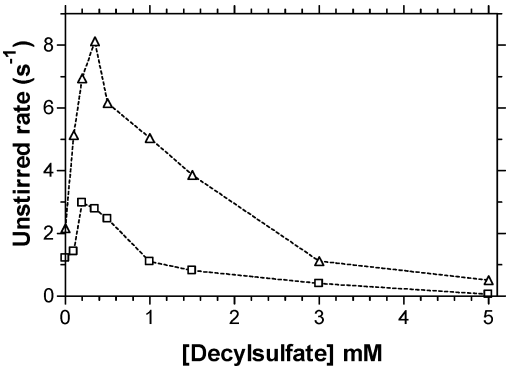

FIGURE 8: Observed rate of hydrolysis of (□) 0.25 or (△) 1 mM DC_7PC by PLA2 in unstirred buffer at pH 7.5. These rates were monitored as the pH-dependent change in the fluorescence of 1 μM pyranine (8-hydroxypyrene-1,3,8-trisulfonic acid) by the protocols described previously (*24*).

(not shown) for the concentration dependence of MJ72 suggest that the level of i-face binding is determined by the sum of concentrations of all amphiphiles in solution. These results were not analyzed further because at this stage we do not have an adequate understanding of the relative partitioning and binding of amphiphiles clustered on the i-face of the complexes, and of their effect on the intensity values.

Catalytic Turnover by $E_i^{\#}S$ Complexes of PLA2. The effect of the active site-directed *sn*-2-amide (PCU or PGU) or *sn*-2-tetrahedral (MG14, MJ72, and MJ33) substrate mimicking the amphiphile binding to the i-face shows that these mimics bind to the active site of the premicellar complexes of PLA2. Similar $E_i^{\#}S$ complexes are likely to be formed in the presence of monodisperse substrate. As shown in Figure 8, the observed rate with monodisperse DC_7PC (CMC = 1.5 mM) alone is estimated to be <0.1 s^{-1} under unstirred conditions where there is little contribution from the reaction on the walls of the reaction chamber or the formation of the premicellar complex with the substrate alone (*24*). It suggests that catalytic efficiency of monodisperse ES is exceedingly low. The rate change with added decylsulfate is biphasic. Superficially, it suggests that the rate of turnover with $E_1^{\#}S$ is highest and that $E_2^{\#}S$ and $E_3^{\#}S$ complexes are catalytically less efficient. However, under these kinetic assay conditions, if the first complex is already formed with the monomer DC_7PC in the absence of decylsulfate, the rate in the presence of decylsulfate may be catalyzed by the second complex followed by the rate decrease with the formation of the third complex. Thus, the biphasic effects of added decylsulfate in Figure 8 may be related to the changes in active site binding, P_b, shown in Figure 6 as developed in the Appendix.

According to this interpretation, the premicellar $\tilde{E}_2^{\#}S$ Michaelis complex has another bound substrate molecule. The peak rate catalyzed by $\tilde{E}_2^{\#}S$ is ~ 8 s^{-1} compared to the rate of ~ 15 s^{-1} for DC_7PC micelles in 1 mM NaCl. Also, the turnover rate is 660 s^{-1} for DC_7PC micelles in 4 M NaCl (*6, 32, 33*) compared to 270 s^{-1} for anionic DMPM vesicles (*4, 34*). This 30−45-fold rate activation is attributed to the k_{cat}* activation by the anionic charge on the interface (*7, 8*). These results suggest that decylsulfate at higher concentrations may compete with the second substrate bound to $\tilde{E}_2^{\#}S$. The reduced catalytic efficiency of $E_2^{\#}S$, where the second S bound to $\tilde{E}_2^{\#}S$ is replaced with decylsulfate, raises the possibility that the second substrate molecules may be poised to enter the active site in the next processive turnover cycle.

DISCUSSION

Analysis of the results with premicellar complexes permitted dissection of some of the elementary steps of Schemes 1−3. The key result is that the occupancy of the active site activates the binding of amphiphiles to the i-face, and conversely, the binding of amphiphiles to the i-face also promotes the binding of I to the active site. The largest activating effect is in the $E_2^{\#}$ or $\tilde{E}_2^{\#}$ premicellar complex which may be a surrogate for a key functional state between E and interfacial E*. In principle, the coupling between the binding at the i-face and at the active site could be due to direct interactions between amphiphiles at the two sites or a consequence of an allosteric change where binding at either site promotes an enzyme conformation that also binds better at the other site. These two possibilities are not mutually incompatible. In view of the results for the PLA2 mutants with impaired coupling in the following paper (*19*), the coupling between the calcium-dependent binding of an inhibitor to the active site of PLA2 and the binding of an amphiphile to the i-face is interpreted as being allosteric. The significance of the results with premicellar complexes and the associated model developed in the Appendix are discussed below in relation to the allosteric K_S* (*5, 6*) and k_{cat}* (*7, 8*) activation by the interface.

Allosteric Coupling of the Active Site and i-Face Events. Monodisperse zwitterionic PCU binds cooperatively to the i-face to form premicellar complexes $\tilde{E}_1$ and $\tilde{E}_2$ (Scheme 2). The first step could involve a single molecule, or possibly a few with weak cooperativity. The second step involves some clustering of a number of PCU molecules on the i-face which does not require calcium. In the presence of calcium, PCU binds to the active site and the i-face binding is significantly altered, both for PCU and for decylsulfate.

Analysis of the titration curves in Figures 1 and 5 shows that most of the Trp signal variation comes from the cooperative amphiphile binding to the i-face in $E_2^{\#}$ complexes with a Hill number of 2−5 for PCU on the i-face, or 6−8 if PCU is also at the active site. In comparison, the Hill number is 6−8 for decylsulfate alone or with PCU at the active site. Here the most significant result is that decylsulfate forms $E_2^{\#}$, for which the dissociation constant decreases with the binding of PCU to the active site. Also, as expected from the thermodynamic reciprocity of the allosteric coupling, the apparent dissociation constant for PCU bound to the active site of $\tilde{E}_2^{\#}I$ or $\tilde{E}_2I$ is lower than for the EI, $E_1^{\#}I$, or $\tilde{E}_1I$ form (Figure 6), and further change is also possible with the formation of $E_3^{\#}$. Ignoring some minor effects whose origin is not clear, we find that the binding parameters for the $\tilde{E}_1^{\#}I$ complex show that the binding of PCU to the i-face and also to the active site to form $\tilde{E}_1I$ promotes further cooperative binding of PCU or decylsulfate to the i-face for formation of $E_2^{\#}I$ or $\tilde{E}_2^{\#}I$. In spite of the uncertainty in the details, the results clearly demonstrate the rich potential for regulation that is afforded by such coupling between the i-face and the active site interactions.

Outlook for Interfacial Activation. We suggest that $\tilde{E}_2^{\#}I$ with a higher affinity for the active site is a proxy for the interface-activated PLA2. As shown before, one subunit of

PLA2 is fully catalytically active for the processive turnover at the interface (*35*). Our analysis in the Appendix suggests that the activation requires binding of two PCU molecules per enzyme. The $\tilde{E}_2^{\#}I$ complex with two PCU molecules bound per enzyme is different from the ternary EI_2 complex invoked in the dual-phospholipid model where binding of a monomeric *sn*-2-amide mimic of the substrate to a regulatory site on monomeric IA PLA2 (*Naja naja naja*) activates the binding of a second inhibitor molecule to the active site (*36, 37*). Our results show that the level of PCU binding to the active site of pig pancreatic IB PLA2 increases primarily after the formation of a premicellar complex $\tilde{E}_2^{\#}I$ with a Hill number of 4−8 and the bound amphiphiles are clustered. It suggests another interpretation of the results of Dennis et al. obtained in the presence of Triton X-100 (*36, 37*): it is likely that the EI_2 complex that is conceived by Dennis et al. with only two bound mimic molecules also contains some bound detergent. If this complex with Triton X-100 is similar to our $\tilde{E}_2^{\#}I$, its formation would be accompanied by an increase in active site affinity. With this possibility, the first i-face binding of PCU ($\tilde{E}_1$) that we observe may correspond to the binding of inhibitor (or substrate) to a regulatory site, while full activation requires more amphiphiles bound at the i-face.

$\tilde{E}_2^{\#}I$ and $\tilde{E}_2^{\#}S$ could be a proxy for the K_S*-activated Michaelis−Menten complex, E*S, in which in addition to the substrate molecule bound to the active site, another may be bound to a regulatory site, and this complex is stabilized by interaction of other amphiphiles with the i-face. For example, the Michaelis complex for the cholate-activated interfacial turnover by PLA2 would contain five or six cholate molecules bound in addition to the substrate molecules at the active site and the regulatory site (*20*). In this model, the rate-lowering effect of certain bile salts (*20*) or cembrenes (*38, 39*) is attributed to the competition for the substrate bound to the regulatory site, which will lower the processive turnover rate. As also observed experimentally, such a rate lowering effect depends on the mole fraction of the rate lowering compound; however, it is not due to the surface dilution of the substrate. This regulatory mechanism accounts not only for the rate decrease at higher decylsulfate concentrations (Figure 8) but also for the wide-ranging quality of interface effects, including those on the ranges of the interfacial activation factors as discussed in the Appendix and also in the following paper (*19*).

APPENDIX

PCU Binding. Specific steps within the paradigm of Scheme 2 are modeled for PLA2 under experimentally established boundary conditions where discrete premicellar complexes form. In the absence of calcium (first row), the PCU amphiphile binds only to the i-face to form first $\tilde{E}_1$ with Hill number $\tilde{n}_1$ and then $\tilde{E}_2$ with Hill number $\tilde{n}_2''$ at the higher PCU concentration. In the presence of calcium bound to the active site (second row), PCU inhibitor (I) also binds to the active site to form EI, $\tilde{E}_1I$, and $\tilde{E}_2I$ complexes (third row). Thus, in the presence of EGTA, only the first row of i-face binding states will be present and contribute to the Trp-3 signal. They are assumed to have signals A_0, B_1, and C_2, respectively. Calcium, when present, binds to the catalytic site in a manner independent of the i-face events. Calcium binding as such does not significantly (<5%) influence the emission of Trp-3 from E (*19*), and possibly not from the other complexes either. Therefore, the three states in the middle row are also assumed to have signals A_0, B_1, and C_2, respectively. I binds to the catalytic site only when calcium is bound, and the three states in the bottom row are assumed to have Trp signals A_0^I, B_1^I, and C_2^I, respectively. Thus, Scheme 2 gives a total Trp signal as a function of added I, at concentration I, as

$$F(C,I)=\frac{1}{Z(C,I)}\left(A_0+A_0^I\frac{IC}{K_I}+\left(\frac{I}{\tilde{K}_1''}\right)^{\tilde{n}_1}\left\{B_1+C_2\left(\frac{I}{\tilde{K}_2''}\right)^{\tilde{n}_2''}+\frac{IC}{\tilde{K}_I}\left[B_1^I+C_2^I\left(\frac{I}{\tilde{K}_2'''}\right)^{\tilde{n}_2'''}\right]\right\}\right) \quad (1)$$

where

$$Z(C,I)=1+\frac{IC}{K_I}+\left(\frac{I}{\tilde{K}_1''}\right)^{\tilde{n}_1}\left\{1+\left(\frac{I}{\tilde{K}_2''}\right)^{\tilde{n}_2''}+\frac{IC}{\tilde{K}_I}\left[1+\left(\frac{I}{\tilde{K}_2'''}\right)^{\tilde{n}_2'''}\right]\right\} \quad (2)$$

and C is determined from the calcium concentration as

$$C=\frac{[Ca]}{[Ca]+K_{Ca}} \quad (3)$$

That is, $C = 0.59$ at 0.5 mM Ca for $K_{Ca} = 0.35$ mM (*18*). Setting C equal to 1 corresponds to the case when the active site is saturated by calcium and only the two bottom rows in Scheme 2 contribute.

Fitting the experimental curves in Figure 1 in the presence and absence of calcium with this model allows identification of the binding parameters. The curve with EGTA in Figure 1 looks nearly hyperbolic, suggestive of a single binding step. However, on the basis of results in this paper and also in analogy with the behavior with decylsulfate (*11, 15*−*17*), assuming a two-step binding leads to a significant improvement in the fit, the mean-square deviations between data points and the best-fit curve decrease by a factor of 5. The fit shown in Figure 1 with EGTA (i.e., setting C equal to 0 in the equations given above) corresponds to the best-fit parameter values: $\tilde{K}_1'' = 60$ μM, $\tilde{K}_2'' = 77$ μM, $\tilde{n}_1 = 1$, $\tilde{n}_2'' = 3.1$, $A_0 = 32.5$, $B_1 = 45$, and $C_2 = 45$. The two steps are better resolved with decylsulfate (*11*) than with PCU. As also shown later and elsewhere (*25*), the magnitude of the intensity change depends on the headgroup of the amphiphile. There is significant uncertainty and covariation in some of these fit parameters. To estimate ranges, we looked for best fits where all but one of the parameters were varied; the one not varied was locked at a value where the best fit with the remaining parameters increased the mean-square deviations by 50%. This procedure gave the following extreme ranges: $\tilde{K}_1'' = 10-2000$ μM, $\tilde{K}_2'' = 30-100$ μM, $\tilde{n}_1 = 0.7-1.6$, $\tilde{n}_2'' = 1.6-5.4$, $B_1 = 36-91$, and $C_2 = 42-46$. Not unexpectedly, there are strong covariations in $\tilde{K}_1''$, $\tilde{n}_1$, and B_1.

Accepting these best-fit numbers in EGTA, we can fit the rest of the parameters in Scheme 2 using the data in the presence of 0.5 mM Ca (Figure 1). Ranges of the parameter values that gave mean-square deviations within 50% above the best fit were as follows: $\tilde{K}_2 = 45-100$ μM, $\tilde{n}_2 = 6-8$, $B_1^I = 25-90$, and $C_2^I = 72-74$. The values of K_I, $\tilde{K}_I$, and A_0^I are virtually indeterminate from these fits as variations in them lead to very small differences in the best fits. While

these ranges do not allow us to pinpoint the parameter values with any accuracy, virtually all fits predict the same qualitative binding behavior: PCU binding to the i-face is influenced by PCU binding to the active site and vice versa. If a 2-fold increase in the mean-square deviations from the best fit is permitted, there exists a narrow region in parameter space where the results in Figure 1 could possibly be fitted without cooperativity between i-face and active site binding. However, this limit also impairs the fits to Figures 2 and 5 discussed below.

These binding parameters deduced from Figure 1 can be used also to interpret the protection data in Figure 2. The rates of inactivation for the complexes in the top row in Scheme 2 are assumed to be k_0, k_1, and k_2; for the middle row k_C, k_{1C}, and k_{2C}; and for the bottom row k_I, k_{1I}, and k_{2I}. The overall inactivation rate follows from eq 1, where the Trp signals for the nine different states are replaced by the corresponding k values. The experimental data in Figure 2 have been fitted using the following relative rates: $k_0 = k_1 = 1$, $k_2 = 0.735$, and $k_C = k_{1C} = k_I = k_{1I} = k_{2C} = k_{2I} = 0.05$. It is expected that the states with bound Ca^{2+}, i.e., the two bottom rows, are protected against alkylation. On the other hand, increasing the amount of PCU seems to lead to a leveling off of the alkylation time, rather than a continued increase. This can be accommodated if the $\tilde{E}_2I$ and possibly $\tilde{E}_2Ca$ states allow a finite rate of alkylation ($k_{2I} > 0$). Introducing small leaks (<5%) in the protection of the other Ca-bound states has little effect on the curve fitting. Adjusting k_2 to <1 and adjusting k_{2I} to >0 are the minimum changes needed to accommodate the experimental data.

Decylsulfate Binding in the Presence of PCU. Scheme 3 is the minimal scheme consistent with the titrations of PLA2 and PCU with decylsulfate (Figure 5), and also the titration of PLA2 and decylsulfate with PCU (results not shown). For the interpretation of results in Figure 5, the horizontal binding steps show binding of decylsulfate while the vertical steps show the binding of PCU (=I) both to the i-face ($\tilde{E}_1$) and to the catalytic site (EI, $E_1^{\#}I$, and $\tilde{E}_i^{\#}I$). As in Scheme 1 in the second row, monodisperse decylsulfate (A) binds only to the i-face to form the three $E_i^{\#}$ (i = 1, 2, or 3) complexes in steps discerned by the change in the Trp-3 fluorescence intensity (*11*). The first column in Scheme 3 is a compacted version of Scheme 2. Furthermore, it is assumed that PCU at sufficiently low concentrations does not participate in the formation of $E_2^{\#}$. Thus, $\tilde{E}_2^{\#}$ and $\tilde{E}_3^{\#}$ denote the states in which PCU forms the first premicellar complex and decylsulfate clustered on the i-face completes the second and third complexes, respectively. PCU binds to the catalytic site only when Ca^{2+} is bound. If calcium has no other effects, like in Scheme 2, the effect of calcium on the active site binding of I can be incorporated by using effective dissociation constants for PCU binding to E and $\tilde{E}_1^{\#}$ of K_I/C and $\tilde{K}_i/C$, respectively, where C is given by eq 3. The Trp signals from the various states in Scheme 3 are assumed to be A_0^I, A_1^I, A_2^I, and A_3^I in the top row and A_0, A_1, A_2, and A_3; B_1, B_2, and B_3; and B_1^I, B_2^I, and B_3^I in the rows below, respectively. The total weighted signal from all 14 states in Scheme 3 can be expressed as

$$F = \frac{(CI/K_I)F_1 + F_2 + (I/\tilde{K}_1'')[F_3 + (CI/\tilde{K}_I)F_4]}{Z} \quad (4)$$

where

$$F_1 = A_0^I + (A/K_1')^{n_1'}\{A_1^I + (A/K_2')^{n_2'}[A_2^I + (A/K_3')^{n_3'}A_3^I]\} \quad (5)$$

$$F_2 = A_0 + (A/K_1^{\#})^{n_1}\{A_1 + (A/K_2^{\#})^{n_2}[A_2 + (A/K_3^{\#})^{n_3}A_3]\} \quad (6)$$

$$F_3 = B_1 + (A/K_2'')^{n_2''}[B_2 + (A/K_3'')^{n_3''}B_3] \quad (7)$$

$$F_4 = B_1^I + (A/K_2''')^{n_2'''}[B_2^I + (A/K_3''')^{n_3'''}B_3^I] \quad (8)$$

The normalization factor (binding polynomial) is

$$Z = (CI/K_I)Z_1 + Z_2 + (I/\tilde{K}_1'')[Z_3 + (CI/\tilde{K}_I)Z_4] \quad (9)$$

where each of the Z_i factors is given by the expression for F_i (eqs 5−8) when all signals (A_i, A_i^I, B_i, and B_i^I) are set to 1. In these equations, I and A are the concentrations of free PCU and free monodisperse decylsulfate, respectively.

While in principle one can imagine other states, e.g., where the premicellar complexes include variable numbers of PCU and decylsulfate mixed together on the i-face, this would introduce many more parameters. The only i-face mixing allowed in Scheme 3 is where PCU forms the first premicellar state and then decylsulfate can complete the second and third, as shown in the two bottom rows. Apart from the 15 parameter values taken from the fits in Figure 1 and from the fit without PCU in Figure 5, which we assume to be established independently, there are 22 new parameters to adjust to produce fits to the four curves with PCU in Figure 5. Exploring the whole solution space with all possible ranges of all parameters does not seem feasible. The main point is that it works. Furthermore, good fits can be achieved under different constraints, and therefore, there are not sufficient data to identify all parameters even for this minimal scheme. Also, there is no evidence to introduce and support a more elaborate scheme.

All variations in parameters we have tried that reasonably fit the data lead to the same qualitative interpretation: There is a strong cooperativity between the binding of PCU in the active site and the formation of the $E_2^{\#}$ and/or $\tilde{E}_2^{\#}$ premicellar complexes. There are in principle two ways that this can occur. Either there is a general coupling between binding at the active site and at the i-face, such that when the second premicellar complex forms, binding at the active site also becomes more favorable. Or there is a specific cooperativity such that PCU binding at the i-face stabilizes formation of $\tilde{E}_2^{\#}$ with both decylsulfate and PCU binding in the active site. As a consequence, increasing decylsulfate concentrations will stabilize PCU binding at the i-face (or a regulatory site) which, in turn, will stabilize binding of the second PCU at the active site. By constraining various sets of parameters in Scheme 3, we could carry out optimal fitting in a number of different cases. In all fits that we have found, there is a strong activation of the formation of the second premicellar complex from PCU binding both at the i-face and at the active site ($A2_{ia} = K_2^{\#}/K_2''' \sim 8$). What is not certain is how this effect is subdivided between the effects of having PCU bound only at the active site ($A2_a = K_2^{\#}/K_2'$) versus PCU only at the i-face ($A2_i = K_2^{\#}/K_2''$). It is not possible from these results to determine which form of cooperativity dominates. Some of the limiting cases shown in Figure 6 are outlined below.

(1) The dashed curve in Figure 6 is based on the assumption that the i-face binding of decylsulfate and PCU in the first complex has the same effects both on the Trp signal and on the formation of the higher premicellar complexes. Thus, the parameters of rows 1 and 4 in Scheme 3 are the same, and those of rows 2 and 3 are also the same. In this limit, the fit requires that there be a strong cooperativity between the binding of PCU to the i-face and to the active site manifested as an increased active site affinity for $\tilde{E}_1$ relative to $E_1^{\#}$. For this curve, $A2_a \sim 8$ and $A2_i = 1$; that is, the cooperative effect is only from active site binding. We could not find a good fit under the constraint that the i-face binding of PCU has the same effect as decylsulfate throughout also on the active site affinity.

(2) The dotted curve in Figure 6 is based on the assumption that binding of PCU in the active site does not influence decylsulfate binding, unless PCU is also bound at the i-face; that is, in Scheme 3, rows 1 and 2 are the same while rows 3 and 4 can be different from each other. Thus, PCU in the active site affects the i-face binding of decylsulfate but only when it is also bound at the i-face. For this curve, $A2_a = 1$ and $A2_i \sim 3.5$; that is, the cooperative effect is partially in the i-face binding of PCU but with an extra contribution when PCU is also on the active site ($K_2''/K_2''' \sim 2.5$). We could not find a good fit with the assumption that the binding of PCU at the active site has no direct influence on the binding parameters of decylsulfate in the premicellar complexes, i.e., if the parameters of the horizontal steps would be the same not only in rows 1 and 2 but also in rows 3 and 4.

(3) The overall best fits for the entire data set in Figure 5 are achieved when there is a mixture of these cooperative effects, the specific PCU effect and the general i-face binding effect. The result of one such fit is given by the parameters in Table 1, and the resulting apparent active site affinity is shown as the solid curve in Figure 6. For this curve, $A2_a = 2.5$ and $A2_i \sim 3.5$; that is, there is a cooperative effect from PCU both at the i-face and at the active site. However, we could not find a fit to all five curves in Figure 5 with the assumption that PCU does not bind the i-face, or that PCU on the i-face has no effect on active site binding.

It should be noted that the fitted curves in Figure 5 are based on I representing the free concentration (I_f) of PCU, while for the experimental curves, the given value of I is the total added amount ($I_T = 2$, 5, 7, and 15 μM). The effect of inhibitor depletion is expected to be largest around the formation of $\tilde{E}_2^{\#}I$, where two PCU molecules can be bound per enzyme. While it is cumbersome to introduce depletion in eqs 4−9, it is straightforward to evaluate its effects afterward. Thus, first optimal fitting was carried out as though the measured data were at $I_f = 2$, 5, 7, and 15 μM. With the fitted parameters, the corresponding $I_T = I_f +$ concentration of bound PCU could be calculated, and the predicted signal can also be calculated for the relevant values of I_T. The main effect is that the predicted curves are displaced slightly (ca. 10% at most) toward higher concentrations of decylsulfate, particularly at low values of I_T (2 or 5 μM). Thereafter, parameters could be adjusted by hand to shift the predicted curves back to fit the experimental ones at the given I_T; the main change needed is a ca. 10% decrease in K_2. Since these parameter adjustments are much smaller than the several-fold effects upon which we are focusing, we did not pursue this kind of correction in detail. Also, neglecting depletion seems to lead to an underestimate of the thermodynamic coupling between binding at the active site and the i-face, and therefore, the effects reported above are not artifacts of depletion.

We also tried an extended Scheme 3 where formation of $E_1^{\#}$ does not occur on the same site as the i-face binding of PCU; in this case, decylsulfate does not interfere with the activating effect of PCU. The strong increase in active site affinity due to the formation of $E_2^{\#}$ and $\tilde{E}_2^{\#}$ shown in Figure 6 is robust in all variations of Scheme 3 that we have tried.

The predicted downturn of the active site binding in Figure 6 at >2 mM decylsulfate is due to the competition from $E_3^{\#}$ formation. According to Scheme 3 and the parameter values in Table 1, an increasing decylsulfate concentration could compete out PCU from its i-face binding. Thus, $E_3^{\#}$ formation could actually destabilize active site binding, particularly when active site binding depends on having PCU at the i-face. However, properties of $E_3^{\#}$ are extremely uncertain, and other variations of the fit parameters can give a larger or smaller downturn in active site binding at higher concentrations of decylsulfate.

REFERENCES

1. Jain, M. K., Egmond, M. R., Verheij, H. M., Apitz-Castro, R., Dijkman, R., and De Haas, G. H. (1982) Interaction of phospholipase A2 and phospholipid bilayers. *Biochim. Biophys. Acta 688*, 341–348.
2. Apitz-Castro, R., Jain, M. K., and De Haas, G. H. (1982) Origin of the latency phase during the action of phospholipase A2 on unmodified phosphatidylcholine vesicles. *Biochim. Biophys. Acta 688*, 349–356.
3. Jain, M. K., Rogers, J., Jahagirdar, D. V., Marecek, J. F., and Ramirez, F. (1986) Kinetics of interfacial catalysis by phospholipase A2 in intravesicle scooting mode, and heterofusion of anionic and zwitterionic vesicles. *Biochim. Biophys. Acta 860*, 435–447.
4. Berg, O. G., Yu, B. Z., Rogers, J., and Jain, M. K. (1991) Interfacial catalysis by phospholipase A2: Determination of the interfacial kinetic rate constants. *Biochemistry 30*, 7283–7297.
5. Jain, M. K., Yu, B. Z., and Berg, O. G. (1993) Relationship of interfacial equilibria to interfacial activation of phospholipase A2. *Biochemistry 32*, 11319–11329. [Erratum: (1994) *Biochemistry 33*, 8618].
6. Berg, O. G., Rogers, J., Yu, B. Z., Yao, J., Romsted, L. S., and Jain, M. K. (1997) Thermodynamic and kinetic basis of interfacial activation: Resolution of binding and allosteric effects on pancreatic phospholipase A2 at zwitterionic interfaces. *Biochemistry 36*, 14512–14530.
7. Yu, B. Z., Poi, M. J., Ramagopal, U. A., Jain, R., Ramakumar, S., Berg, O. G., Tsai, M. D., Sekar, K., and Jain, M. K. (2000) Structural basis of the anionic interface preference and k_{cat}* activation of pancreatic phospholipase A2. *Biochemistry 39*, 12312–12323.
8. Rogers, J., Yu, B. Z., Tsai, M. D., Berg, O. G., and Jain, M. K. (1998) Cationic residues 53 and 56 control the anion-induced interfacial k_{cat}* activation of pancreatic phospholipase A2. *Biochemistry 37*, 9549–9556.
9. Berg, O. G., Gelb, M. H., Tsai, M. D., and Jain, M. K. (2001) Interfacial enzymology: The secreted phospholipase A2-paradigm. *Chem. Rev. 101*, 2613–2654.
10. Berg, O. G., and Jain, M. K. (2002) *Interfacial Enzyme Kinetics*, Wiley, London.
11. Berg, O. G., Yu, B. Z., Chang, C., Koehler, K. A., and Jain, M. K. (2004) Cooperative binding of monodisperse anionic amphiphiles to the i-face: Phospholipase A2-paradigm for interfacial binding. *Biochemistry 43*, 7999–8013.
12. Yu, B. Z., Berg, O. G., and Jain, M. K. (2007) Role of the 57−72 loop in the cooperative binding of amphiphiles to the i-face of pancreatic IB phospholipase A2. *Biochim. Biophys. Acta* XXXXX.
13. Yu, B. Z., Apitz-Castro, R., Tsai, M. D., and Jain, M. K. (2003) Interaction of monodisperse anionic amphiphiles with the i-face of secreted phospholipase A2. *Biochemistry 42*, 6293–6301.

14. Bai, S., Jain, M. K., and Berg, O. G. (2008) Contiguous binding of decylsulfate on the interface binding surface of pancreatic phospholipase A2. *Biochemistry 47*, 2899–2907.
15. Yu, B. Z., Polenova, T. E., Jain, M. K., and Berg, O. G. (2005) Premicellar complexes of sphingomyelinase mediate enzyme exchange for the stationary phase turnover. *Biochim. Biophys. Acta 1712*, 137–151.
16. Jain, M. K., and Berg, O. G. (2006) Coupling of the i-face and the active site of phospholipase A_2 for interfacial activation. *Curr. Opin. Chem. Biol. 10*, 473–479.
17. Berg, O. G., Yu, B. Z., Apitz-Castro, R. J., and Jain, M. K. (2004) Phosphatidylinositol-specific phospholipase C forms different complexes with monodisperse and micellar phosphatidylcholine. *Biochemistry 43*, 2080–2090.
18. Yu, B. Z., Berg, O. G., and Jain, M. K. (1993) The divalent cation is obligatory for the binding of ligands to the catalytic site of secreted phospholipase A2. *Biochemistry 32*, 6485–6492.
19. Yu, B. Z., Bai, S., Berg, O. G., and Jain, M. K. (2009) The allosteric effect of amphiphile binding to phospholipase A2. *Biochemistry 48*, 3219–3229.
20. Yu, B. Z., Apitz-Castro, R., Jain, M. K., and Berg, O. G. (2007) Role of the 57−72 loop in specific interaction of bile salts with pancreatic IB phospholipase A2: Regulation of fat and cholesterol homeostasis. *Biochim. Biophys. Acta 1768*, 2478–2490.
21. Jain, M. K., Tao, W. J., Rogers, J., Arenson, C., Eibl, H., and Yu, B. Z. (1991) Active-site-directed specific competitive inhibitors of phospholipase A2: Novel transition-state analogues. *Biochemistry 30*, 10256–10268.
22. Thunnissen, M. M., Ab, E., Kalk, K. H., Drenth, J., Dijkstra, B. W., Kuipers, O. P., Dijkman, R., de Haas, G. H., and Verheij, H. M. (1990) X-ray structure of phospholipase A2 complexed with a substrate-derived inhibitor. *Nature 347*, 689–691.
23. de Haas, G. H., Dijkman, R., van Oort, M. G., and Verger, R. (1990) Competitive inhibition of lipolytic enzymes. III. Some acylamino analogues of phospholipids are potent competitive inhibitors of porcine pancreatic phospholipase A2. *Biochim. Biophys. Acta 1043*, 75–82.
24. Yu, B. Z., Berg, O. G., and Jain, M. K. (1999) Hydrolysis of monodisperse phosphatidylcholines by phospholipase A2 occurs on vessel walls and air bubbles. *Biochemistry 38*, 10449–10456.
25. Tsai, Y., Yu, B.-Z., Wang, Y., Chen, J. W., and Jain, M. K. (2006) Desolvation map of the i-face of phospholipase A2. *Biochim. Biophys. Acta 1758*, 653–665.
26. Verheij, H. M., Slotboom, A. J., and de Haas, G. H. (1981) Structure and function of phospholipase A2. *Rev. Physiol. Biochem. Pharmacol. 91*, 91–203.
27. Maliwal, B. P., Yu, B. Z., Szmacinski, H., Squier, T., van Binsbergen, J., Slotboom, A. J., and Jain, M. K. (1994) Functional significance of the conformational dynamics of the N-terminal segment of secreted phospholipase A2 at the interface. *Biochemistry 33*, 4509–4516.
28. Jain, M. K., and Maliwal, B. P. (1985) The environment of tryptophan in pig pancreatic phospholipase A2 bound to bilayers. *Biochim. Biophys. Acta 814*, 135–140.
29. Jain, M. K., and Vaz, W. L. (1987) Dehydration of the lipid-protein microinterface on binding of phospholipase A2 to lipid bilayers. *Biochim. Biophys. Acta 905*, 1–8.
30. Ramirez, F., and Jain, M. K. (1991) Phospholipase A2 at the bilayer interface. *Proteins: Struct., Funct., Genet. 9*, 229–239.
31. Pan, Y. H., Epstein, T. M., Jain, M. K., and Bahnson, B. J. (2001) Five coplanar anion binding sites on one face of phospholipase A2: Relationship to interface binding. *Biochemistry 40*, 609–617.
32. Jain, M. K., and Rogers, J. (1989) Substrate specificity for interfacial catalysis by phospholipase A2 in the scooting mode. *Biochim. Biophys. Acta 1003*, 91–97.
33. Rogers, J., Yu, B. Z., Serves, S. V., Tsivgoulis, G. M., Sotiropoulos, D. N., Ioannou, P. V., and Jain, M. K. (1996) Kinetic basis for the substrate specificity during hydrolysis of phospholipids by secreted phospholipase A2. *Biochemistry 35*, 9375–9384.
34. Jain, M. K., Rogers, J., Berg, O., and Gelb, M. H. (1991) Interfacial catalysis by phospholipase A2: Activation by substrate replenishment. *Biochemistry 30*, 7340–7348.
35. Jain, M. K., Ranadive, G., Yu, B. Z., and Verheij, H. M. (1991) Interfacial catalysis by phospholipase A2: Monomeric enzyme is fully catalytically active at the bilayer interface. *Biochemistry 30*, 7330–7340.
36. Lefkowitz, L. J., Deems, R. A., and Dennis, E. A. (1999) Expression of group IA phospholipase A2 in *Pichia pastoris*: Identification of a phosphatidylcholine activator site using site-directed mutagenesis. *Biochemistry 38*, 14174–14184.
37. Boegeman, S. C., Deems, R. A., and Dennis, E. A. (2004) Phospholipid binding and the activation of group IA secreted phospholipase A2. *Biochemistry 43*, 3907–3916.
38. Bai, S., and Jain, M. K. (2008) ^{1}H and ^{13}C assigments of five cembrenes from guggul. *Magn. Reson. Chem. 46*, 791–793.
39. Yu, B.-Z., Kaimal, R., Bai, S., El Sayed, K. A., Tatulian, S. A., Apitz, R. J., Jain, M. K., Deng, R., and Berg, O. G. (2009) Effect of guggulsterone and cembranoids of *Commiphora mukul* on pancreatic phospholipase A2: Role in hypocholesteremic effect. *J. Nat. Prod. 72*, 24–28.

BI801244U